

Production of Hydrogen and Synthesis gas via Cu-Ni/Al₂O₃ catalyzed gasification of bagasse in supercritical water media

Reza Mehrani^a, Ahmad Tavasoli^{a*}, Mohammad Barati^a, Ali Karimi^b, Masoumeh Ghalbi

Ahangari^b

^a- School of Chemistry, College of Science, University of Tehran, Tehran, Iran

^b- Research Institute of petroleum Industry, National Iranian Oil Company, Tehran, Iran

Abstract

Bagasse as a real biomass was converted to hydrogen rich gas via catalytic supercritical water gasification process. To find the effect of Cu on selectivity of products, Cu promoted Ni- γ -Al₂O₃ catalysts were prepared with 1 to 20wt% Ni and 0.5 to 10wt% Cu loadings via impregnation method. Catalysts were characterized by ICP, BET, XRD, H₂ chemisorption and TEM technique as well CHNS analysis was carried out for elemental analysis of bagasse. The biomass supercritical water gasification process was performed in a batch micro-reactor at 400°C and 240 bars. The total gas yield increased with increasing in Ni and Cu loadings up to 15wt% Ni and 7.5 wt% Cu and became approximately constant. The catalytic process increased hydrogen yield to 9.5, CO yield to 2.2 and light hydrocarbons to 0.59 mmol/g bagasse. Total H₂ selectivity (THS) ratio increased with increasing in Ni and Cu loading reached a maximum at 15%wt Ni and 7.5%wt Cu and then began to decrease.

Keywords: Supercritical water gasification, Bagasse, Hydrogen, selectivity, Nickel, Copper

© 2014 Published by Journal of Nanoanalysis.

1. Introduction

Declining petroleum resources with increasing in its demand by emerging economies as well as environmental concerns about fossil fuels greenhouse emission cause international community decision to develop economical and energy efficient processes for the sustainable production of fuels and chemicals. In this respect, biofuels, especially fuels derived from plant biomass, are the promising sustainable sources for this purpose [1-3].

Gasification is a process in which solid or liquid carbonaceous materials, such as biomass, react with air, oxygen, or steam to produce a gas mixture contains CO, H₂, CO₂, CH₄ and some other gaseous

* Corresponding Author: Email: tavassolia@khayam.ut.ac.ir, Phone: (98)-21-61113643, Fax: (98)-21-66495291

hydrocarbons. Pyrolysis, partial oxidation, and steam reforming are the reactions that can occur in biomass supercritical water gasification (SCWG) process [4,5].

In this process, water has temperature and pressure above 374°C and 22.1MPa and acts as both reactant and reaction medium. The unique solvent properties let supercritical water to solve the major part of biomass and reform it through water - gas shift (producing H₂ and CO₂ from CO and H₂O) and methanation (producing CH₄ and H₂O from CO and H₂) reactions. Hydrogen production from SCWG of bagasse is one of the most interesting fields of study [6,7].

High CO producing due to low rate of water gas shift reaction as well as high operating temperatures of non-catalytic SCWG persuaded researchers to perform the process in presence of catalysts especially heterogeneous ones. Catalysts have been used in SCWG for different goals such as increasing the total gas moles coincided with hydrogen selective gas production. It can be obtained with utilizing catalysts using gasifier active metals promoted with others that can accelerate the water gas shift and prevent or decelerate methanation reactions rates [8,9].

Several metals have been used as biomass gasification catalysts.. Among them,, nickel can be introduced as one of the most interested metals to use in different types of biomass gasification due to it's higher activity and lower price. The metal is a good gasifier catalyst because of its intrinsic tendency to cleave C-O bands. However, this property causes lower hydrogen selectivity [10, 11]. Therefore, several metals have been used as promoters to solve the problem. Cobalt and molybdenum have been tested in this way. They showed increasing effect on hydrogen selective gas production from biomass gasification [12, 13-16]. Also, it has been reported that the promotion of Ni with Sn can reduce methane other light hydrocarbons (LH) generation. The metal prevents C-O band cleavage and accelerates C-C band breaking down and this property results higher hydrogen selectivity [17]. It was found that addition of Cu to Ni catalyst increases the yield of hydrogen production with decreasing the rate of methanation reaction in SCWG of glucose as model biomass [12,18-19].

Plant biomass is a complex material that typically consists of cellulose, hemicelluloses and lignin. Therefore, many researches have studied model compounds; such as cellulose, glucose, xylan, glycerol, p-cresol, and phenol to investigate the supercritical and other hydrothermal gasification processes. Annually, more than six hundred thousand tons of bagasse is burned in Haft Tappe Industries Company in Iran, which creates serious environmental problems and wastes huge amount of energy. Therefore, our research group focused on conversion of bagasse as a real biomass to value added products specially hydrogen and syngas via supercritical water gasification. Cu promoted Ni-based catalysts supported on γ -Al₂O₃ with different metal loadings were prepared with impregnation technique. The catalysts were assessed in a batch micro-reactor for carrying out the SCWG of bagasse.

2. Experimental

2.1. Materials

The bagasse biomass was obtained from Haft-Tappe Industries (Iran). It was shaved and ground to obtain particle sizes less than 1mm. Nickel nitrate hexahydrate, Ni(NO₃)₂.6H₂O, and copper nitrate trihydrate, Cu(NO₃)₂.3H₂O, and Conndea Vista Catalox B γ -alumina (200 m²/g, impurities: Sodium oxide (Na₂O)<0.05 (ppm); Silica (SiO₂)<0.9 (ppm); Sulfate (SO₄)<1.5 (ppm)) were purchased from Sigma-Aldrich Company and used for preparation of the catalysts.

2.2. Catalyst preparation

Prior to catalyst preparation, in order to remove combustible impurities and obtain potentially maximum available surface area, the support was calcined at 500°C for 10h. The catalysts were prepared with wet impregnation method with 1 to 20 %wt. of nickel and 0.5 to 10 %wt. of cupper loadings. Nickel nitrate hexahydrate (Ni(NO₃)₂.6H₂O) and copper nitrate trihydrate (Cu(NO₃)₂.3H₂O) were used as raw materials for catalyst preparation. To obtain 3g of each catalyst, certain amount of nickel and copper salts were dissolved in 100ml deionized water. Support (γ -alumina) was added to the solution and the extra of solvent was evaporated in rotary vacuum evaporator. The catalysts were dried at 120°C for 2h and calcined under argon (Ar) flow at 450°C for 3 h and slowly exposed to atmosphere during the cooling step. The prepared catalysts contain 1, 2.5, 5, 10, 20 wt.% nickel and 0.5, 2.5, 5, 7.5, 10 wt.%, copper loadings. The catalysts nomenclature and compositions are listed in Table 1.

Table 1: Chemical composition and preparation details of the calcined catalysts

Sample	Ni Targeted composition (wt.%)	Cu Targeted composition (wt.%)	Ni Measured composition (wt.%)	Cu Measured composition (wt.%)
IMC1	2.5	1	2.38	0.96
IMC2	5	2.5	4.75	2.38
IMC3	10	5	9.80	4.93
IMC4	15	7.5	14.85	7.37
IMC5	20	10	19.60	9.95

2.3. Catalyst characterization techniques

The metal loadings of the calcined catalysts were performed using Varian VISTA-MPX inductively coupled plasma-optical emission spectrometry (ICP-OES) instrument.

Surface area, pore volume and pores average diameter of the calcined catalysts was measured using an ASAP-2020 V2 Micrometrics system. The samples were degassed at 200°C for 4h under 50 mTorr vacuums and their BET surface area, pore volume and pore diameter was determined. The morphology of the calcined catalysts was studied by transmission electron microscopy (TEM). Sample specimens for TEM studies were prepared by ultrasonic dispersion of the catalysts in ethanol, and the suspensions were dropped onto a carbon-coated copper grid. TEM investigations were carried out using a Philips CM20 (100 kV) transmission electron microscope equipped with a NARON energy-dispersive spectrometer with a germanium detector.

Philips Analytical X-ray diffractometer (XPert MPD) with monochromatized Cu/K α radiation, 2 θ angles from 10° to 90° was used to phase analyzing of prepared catalysts. The nickel average crystallite sizes were calculated regarding to its sharpest proprietary XRD peaks and Debye –Scherrer equation.

The amount of chemisorbed hydrogen on the catalysts was measured using the Micromeritics TPD-TPR 290 system. 0.25 g of the sample was reduced under hydrogen flow at 350°C for 4 h and then cooled to 100°C under hydrogen flow. Then the flow of hydrogen was switched to argon at the same temperature, which lasted about 30 min in order to remove the weakly adsorbed hydrogen. Afterwards, the temperature programmed desorption (TPD) of the samples was obtained by increasing the temperature of the samples, with a ramp rate of 10°C/min, to 350°C under the argon flow. The TPD profile was used to determine the metal dispersion and its surface average crystallite size. After the TPD of hydrogen, the sample was re-oxidized at 350°C by pulses of 10% oxygen in helium to determine the extent of reduction. The calculations are summarized below.

$$\begin{aligned} \% \text{Dispersion} &= \frac{H_2 \text{ uptake} \times \text{atomic weight} \times \text{stoichiometry}}{\% \text{metal}} \\ &= \frac{\text{number of Ni}^0 \text{ atoms on the surface} \times 100}{\text{total number of Ni}^0 \text{ atom}} \end{aligned} \quad (1)$$

$$\text{Fraction reduced} = \frac{O_2 \text{ uptake (moles/ g.cat.)} \times \text{atomic weight}}{\text{Percentage metal}} \quad (2)$$

$$\text{Diameter (nm)} = \frac{6000}{\text{density} \times \text{maximum area} \times \text{dispersion}} \quad (3)$$

Table 2: CHNS analysis of biomass species

N	0.69
C	58.1
H	6.45
S	0.19
O	34.57

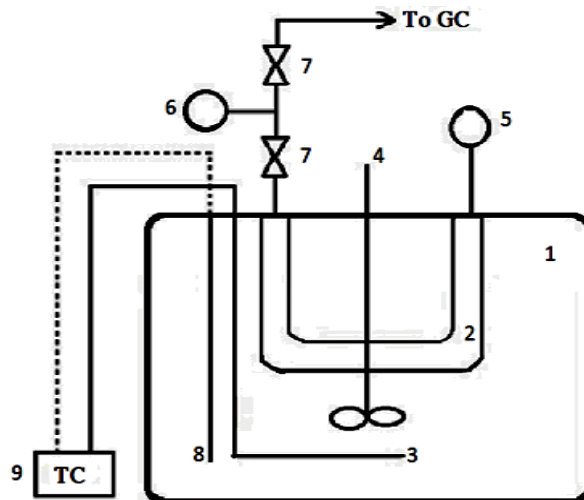


Figure 1: Scheme of the home made tube batch microreactor: 1) molten salt bath, 2) batch tube reactor, 3) electrical heater, 4) mixer, 5) high pressure gauge, 6) low-pressure gauge, 7) high-pressure valve, 8) k-type thermocouple, 9) PID temperature controller.

2.4. Experimental outline

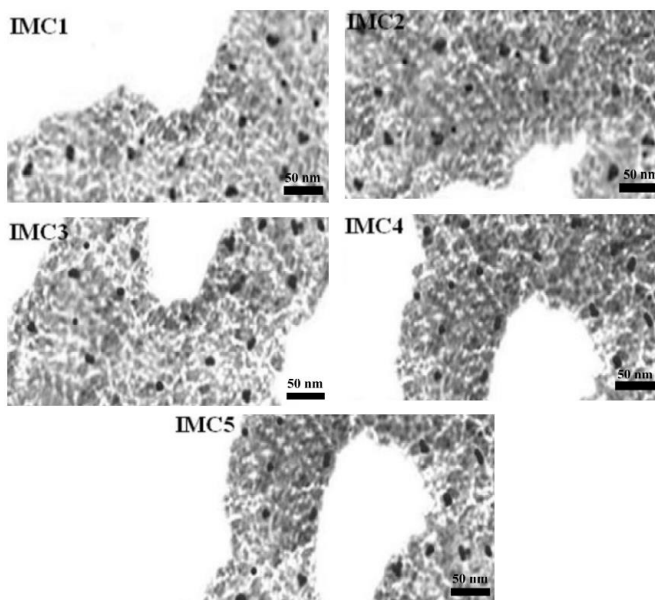
A batch micro reactor made of 316 stainless steel tube with total volume of 25 ml has been used in this study (Figure 1). The process was carried out in presence of as well as without catalyst. For non-catalytic test, 0.08g of bagasse was mixed with a certain amount of deionized water and injected into the reactor using a syringe. The reactor was plunged in a molten salt bath that contains a mixture of potassium nitrate, sodium nitrate and sodium nitrite. The molten salt bath temperature was controlled using an electrical heater and a PID temperature controller. Temperature and pressure were measured using a K-type thermocouple and a high pressure gauge. After 15min reaction time, the reactor was taken out of the molten salt bath and plunged in a water bath for rapid cooling to room temperature. For catalytic tests, certain amount of catalyst is charged to the reactor. The catalyst was then reduced in flowing hydrogen for 4 h at 350°C (50 ml STP/min H₂) before addition of bagasse and deionized water. All experiments were performed 3 times under the same experimental conditions and the data reported here are the averages of repetitive runs. At the end of each experiment, reactor free volume, final pressure and temperature were used to calculate amount of gas yield. Produced gases were analyzed using gas chromatographs (Varian 3400 and Teyfgostar-Compact) to find their components quantitatively and qualitatively. For each experiment, the carbon gasification ratio (CGR) which is the ratio of the amount of carbon in the gaseous products to the amount of carbon in the bagasse and hydrogen gasification ratio (HGR) which is the ratio of the amount of hydrogen in the gas phase to the amount of hydrogen in the bagasse were measured after each experiment. Mathematically, CGR and HGR are defined as:

$$\text{CGR} = \frac{\{Y_{\text{CO}} + Y_{\text{CH}_4} + Y_{\text{CO}_2} + 2Y_{\text{C}_2\text{H}_4} + 2Y_{\text{C}_2\text{H}_6}\}}{\{\text{mmol Carbon / g bagasse}\}} \quad (4)$$

$$\text{HGR} = \frac{\{Y_{\text{H}_2} + 2Y_{\text{CH}_4} + 2Y_{\text{C}_2\text{H}_4} + 3Y_{\text{C}_2\text{H}_6}\}}{\{\text{mmol H}_2 \text{ / g bagasse}\}} \quad (5)$$

Table 3: Textural properties of the calcined catalysts.

Sample	BET surface area (m ² /g)	Total pore volume (ml/g)	Average pore diameter (Å)
Support	275.6	0.758	11
IMC1	241.7	0.603	11.7
IMC2	224.3	0.588	11.9
IMC3	197.3	0.537	12
IMC4	161.7	0.499	12.1
IMC5	137.7	0.450	12.3

**Figure 2:** TEM micrographs of calcined catalysts.

3. Results and discussion

3.1. Biomass CHNS analysis

The CHNSO elemental analysis results (Table 2) showed that the carbon, hydrogen, oxygen, sulphur and nitrogen content of dry biomass were 58.1%; 6.45%; 34.57%, 0.19% and 0.69%, respectively.

3.2. Catalysts characterization

The elemental compositions of the calcined catalysts measured by ICP are given in Table 1. This table shows that the metal contents of the catalysts were fairly similar and close to the targeted metal contents. Results of surface area measurement for calcined catalysts are given in Table 3. The results interpret more pore blockage by metal oxide clusters in the catalysts having higher metal loadings because of decreasing in BET surface area with increasing the loadings. Data on this table also shows a decreasing in total pore volume of the catalysts with increasing the metal loadings, significantly.

The TEM micrographs of IMC₁-IMC₅ catalysts are shown in Figure 2. Figure shows particles distribution on surface of the support pores. The micrographs confirm metal particles precipitation in nano pores through impregnating them into γ -Al₂O₃. This figure also shows slight population increasing of nanoparticles from IMC₁ to IMC₂.

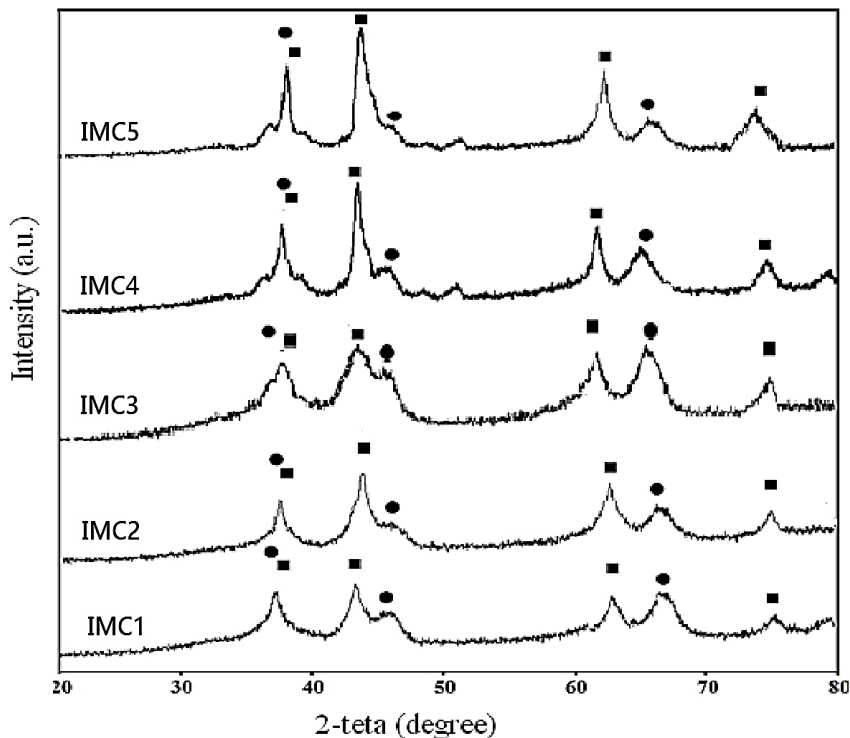


Figure 3: XRD patterns of calcined catalysts.

To determine the crystalline phases, X-ray diffraction experiments (XRD) of the calcined catalysts were performed. XRD patterns of the catalysts are shown on Figure 3. According to XRD patterns, the peaks at 2θ values of 36.5° , 46° and 66.7° correspond to the support, while the other peaks are related to different crystal planes of nickel oxide (peaks at 2θ values of 37.1° , 43.3° , 63° and 75.6°). The average nickel oxide crystallite sizes for the catalysts were calculated using Debye-Scherrer equation and the line broadening at the half height of Ni peak with maximum intensity which is the peak at $2\theta = 43.3^\circ$. Results are shown on Table 4. The calculations revealed that crystallite size increases with increasing metal loadings.

The results of H_2 chemisorption tests are given on Table 5. This table shows that, increasing metal loadings considerably decreases percentage dispersion. By increasing the metal loadings, the average particles diameter increased from 4.9 to 13.5 nm. Also, the percentage reduction of the catalysts shows considerable increase which is due to easier reduction of larger particles. Higher dispersion in case of catalysts prepared with lower metal loadings increases the interactions between the active metal and as a result decreases the percentage reduction.

Table 4: Particle sizes of the calcined catalysts.

Catalyst	dp(nm) calculated by Debye-Scherer formula
IMC1	5.1
IMC2	6.4
IMC3	7.9
IMC4	11
IMC5	13.6

Table 5: H₂ chemisorption results for the calcined catalysts.

Catalyst	%Reduction	% Dispersion	dP (nm)
IMC1	37.1	51.2	4.9
IMC2	45.8	39.5	6.3
IMC3	50.1	30.8	7.6
IMC4	52.14	17.6	10.6
IMC5	55.07	9.7	13.5

Table 6: The non-catalytic gasification yields (mmol of gas /g of bagasse) for the whole gaseous products and H₂, CO, CO₂ and light hydrocarbons (T=400°C, Reaction time= 15 min, bagasse loading: 0.08 g, water loading: 6.5 g).

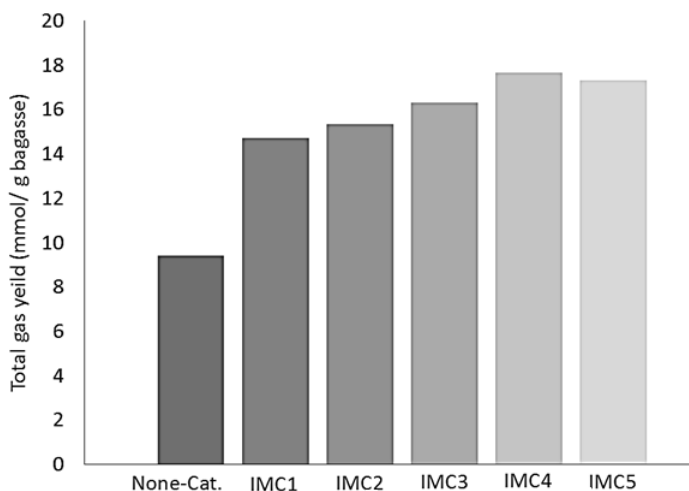
Total gas	9.41
H ₂	3.34
CO ₂	4.57
CO	1.75
Light hydrocarbons	0.51

3.3. Reaction

3.3.1. Non-catalytic gasification

Non-catalytic SCWG of bagasse was preceded at reaction condition noted previously. Table 6 presents the gasification yields (mmol of gas/g of bagasse) for the whole gaseous products and H₂, CO, CO₂ and light gaseous hydrocarbons.

It is referred by different authors that, biomass gasification in SCWG is a complex process, but the overall chemical conversion can be represented by the simplified net reaction:

**Figure 4:** Total gas yields for non-catalytic and IMC₁-IMC₅ catalyzed SCWG of bagasse and for the catalysts prepared by impregnation method (T: 400°C, reaction time: 15 min, bagasse loading: 0.08 g, water loading: 6.5 g).

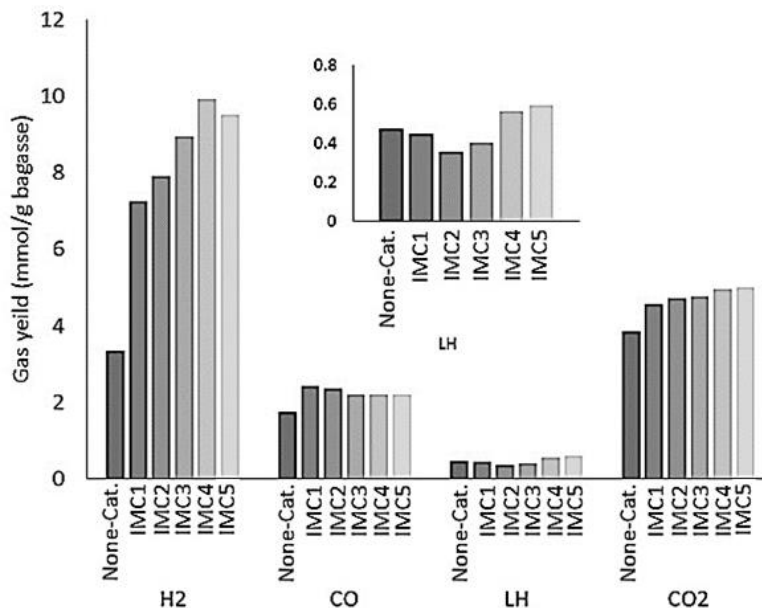
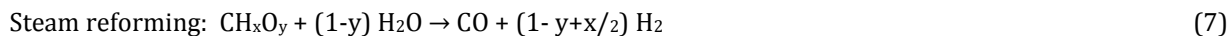


Figure 5: Composition of produced gases for non-catalytic and IMC1- IMC5 catalyzed SCWG of bagasse (T: 400 oC, Reaction time: 15 min, bagasse loading: 0.08 g, water loading: 6.5 g).

Where x and y are the elemental molar ratios of H/C and O/C in biomass, respectively. Reaction (6) is an endothermic reaction. It is known from reaction (6) that water is not only the solvent but also a reactant and the hydrogen atoms in the water is released as hydrogen gas through the reaction. Equation (6) summarizes the overall reaction, but a group of competing intermediate reactions, which are essential for the successful gasification; need to be considered as follows:



The results on Table 6 shows that, the final product gas composition of the bagasse SCWG is a result of combination of the above mentioned series of complex and competing reactions.

3.3.2. Catalytic gasification

Catalytic experiments were carried out with catalysts prepared via impregnation method at noted reaction condition. Figure 4 compares the total gas yields (mmol of gas/g of bagasse) of catalytic and non-catalytic processes. Results showed that addition of catalyst increases the gas production from 9.4 for noncatalytic process to 17.3 mmol/g bagasse for IMC₅. However, increasing Ni and Cu loadings as IMC₄ to IMC₅ did not change the total gas yield, significantly. Decreasing in available surface area for dispersing metals in higher loadings and pore blockage can limit producing total gas yield. The figure also shows a mild increasing for CH₄, CO and CO₂ yields and a significant increasing in H₂ yield with increasing in Ni and Cu loadings.

Figure 5 shows the composition of produced gases for the non-catalytic and IMC₁-IMC₅ catalyzed SCWG of bagasse. As shown on this figure, addition of catalyst to process increased all gases yields except LH. After the increasing H₂ had a maximum, LH had a minimum, CO₂ had a mild increasing and CO had a mild decreasing behaviours. It has been shown that Cu decreases the adsorption of hydrogen and carbon monoxide on the catalyst surface. Decrease in adsorption of CO at higher Cu loadings can suppress reaction 9 (methanation) and hence decreases light gaseous hydrocarbons formation rates and increases the hydrogen production yield. Also, it has been shown that Cu can catalyze methane reforming reaction (reaction 7) which can enhance formation rate of hydrogen. Increase in hydrogen moles also can be explained by increasing the rate of water-gas shift reaction (reaction 8) due to increase in the contents of metals in the catalysts.

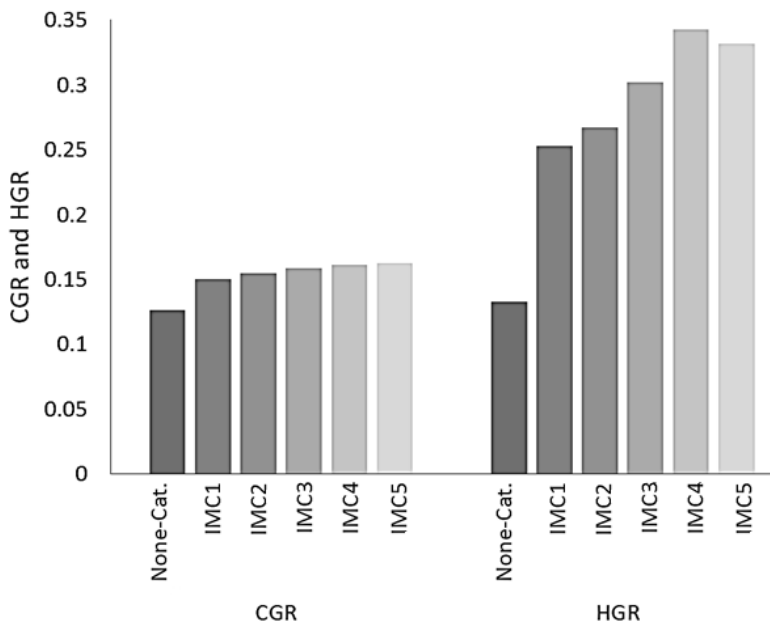


Figure 6: The HGR and CGR for non-catalytic and IMC₁- IMC₅ catalyzed SCWG of bagasse (T: 400°C, Reaction time: 15 min, bagasse loading: 0.08 g, water loading: 6.5 g).

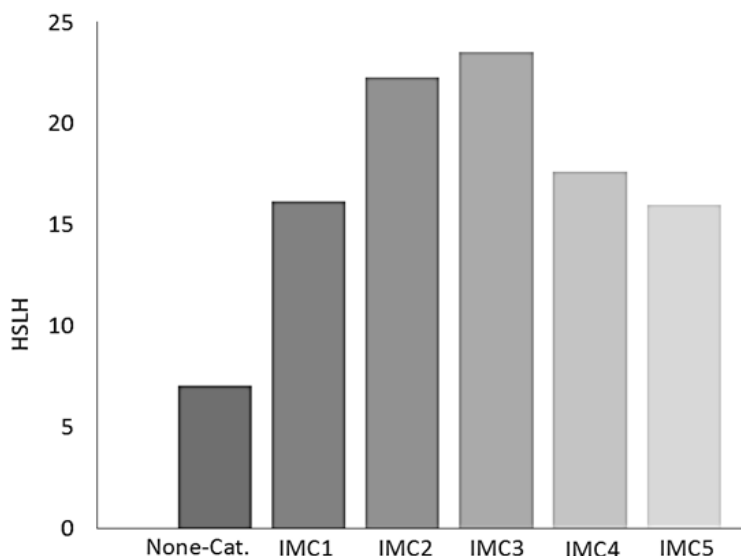


Figure 7: H₂ selectivity to light hydrocarbons (HSLH) for non-catalytic and IMC₁- IMC₅ catalyzed SCWG of bagasse (T: 400°C, Reaction time: 15 min, bagasse loading: 0.08 g, water loading: 6.5 g).

The CGR and HGR values were calculated from the gasification data. The results are shown on Figure 6. As shown, maximum hydrogen gasification ratio of 0.34 is achieved for catalyst prepared with Ni loading of 15 wt.% and Cu loading of 7.5 wt.%. The CGR also had an increasing manner from 0.126 for noncatalytic process to 0.162 for IMC₅. The trend shows this value approximately became constant in higher metal loadings.

Also the relationship between H₂ selectivity and metal loading also was investigated. Two types of hydrogen selectivity were defined to make metal loading effect on hydrogen production more clear. The definitions are presented below as HSLH (H₂ selectivity to light hydrocarbons) and THS (Total H₂ selectivity).

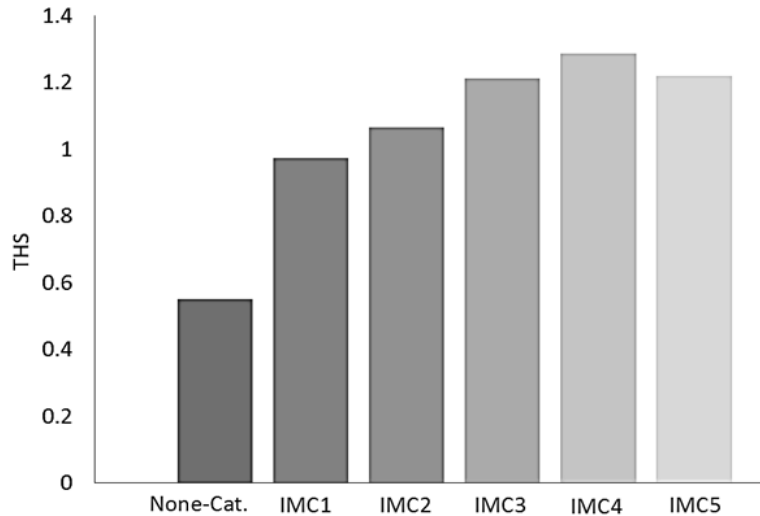


Figure 8: Total H₂ selectivity (THS) for non-catalytic and IMC₁- IMC₅ catalyzed SCWG of bagasse (T: 400°C, Reaction time: 15 min, bagasse loading: 0.08 g, water loading: 6.5 g).

$$\text{HSLH} = \{Y_{\text{H}_2} \text{ (mmol/g bagasse)}\} / \{Y_{\text{LH}} \text{ (mmol/g bagasse)}\} \quad (10)$$

$$\text{THS} = \{Y_{\text{H}_2} \text{ (mmol/g bagasse)}\} / \{Y_{\text{CO}} + Y_{\text{LH}} + Y_{\text{CO}_2} \text{ (mmol/g bagasse)}\} \quad (11)$$

Figure 7 shows H₂ selectivity to light hydrocarbons (HSLH). As shown, there is an optimum value at 5 and 10 weight percents for Cu and Ni loadings, respectively. The initial increasing can be related to nature of Cu in methane reforming and methanation deceleration as well as water gas shift acceleration. After the optimum, HSLH decreasing occurs because of active metals particles agglomeration and subsequently decreasing in active surface area. Total H₂ selectivity (THS) shows in Figure 8. THS had an optimum, and the maximum THS was occurred at 7.5 and 15 weight percents for Cu and Ni, respectively. The manner can be interpreted with arguments similar to HSLH. But, the optimum points are different. The difference can be considered that the catalytic activity missing at higher metal loadings has more intensive undesirable effect on preventing light hydrocarbons production than decreasing produced CO. Decreasing in CO can raise the THS. Therefore declining in its consumption in water gas shift reaction at higher metal loadings of catalyst can reduce THS.

4. Conclusion

SCWG of bagasse was carried out in presence of Ni-Cu/ γ -Al₂O₃ catalysts prepared by impregnation method. These results were compared with non-catalytic reaction. It was found that using Ni-Cu/ γ -Al₂O₃ catalyst significantly increases the H₂ production yield in this process. Maximum total gas yields and maximum hydrogen selectivity were achieved with 15wt.%Ni and 7.5wt.%Cu loadings. Decrease in adsorption of CO at higher Cu loadings can suppress methanation and hence decreases light gaseous hydrocarbons formation rates and increases the hydrogen production yield. Also, it has been shown that Cu can catalyze methane reforming reaction which can enhance formation rate of hydrogen. Increase in hydrogen moles also can be explained by increasing the rate of water-gas shift reaction due to increase in the contents of metals in the catalysts. The HGR values were maximum of 0.34 and the CGR also increased to 0.162 for catalyst prepared with Ni loading of 15 wt.% and Cu loading of 7.5 wt.%. The trend shows the CGR approximately became constant and the HGR decreased in higher metal loadings.

References

- [1] C. E. Zhang, Z. Zhang, M. V. Keitz, K. Valentas, Treatment Variable Effects on Supercritical Gasification of High-Diversity Grassland Perennials, *Applied Biochemistry and Biotechnology*. 154 (2009) 238-245.
- [2] C. E. Wyman, Alternative fuels from biomass and their impact on carbon dioxide accumulation, *Applied Biochemistry and Biotechnology*. 45 (1994) 897-915.
- [3] C. E. Wyman, N. D. Hinman, Ethanol: Fundamentals of Production from, *Applied Biochemistry and*

Biotechnology, 24 (1990) 735-753.

- [4] L. R. Lynd, H. J. Cushman, J. R. Nichols, C. E. Wyman, Fuel Ethanol from Cellulosic Biomass, *Science*, 251 (1991) 1318-1323.
- [5] A. F. Kirkels, G. P.J. Verbon, Biomass gasification: Still promising? A 30-year global overview, *Renewable Sustainable Energy Reviews*, 15 (2011) 471-481.
- [6] M. P. Arnavat, J. C. Bruno, A. Coronas, Review and analysis of biomass gasification models, *Renewable Sustainable Energy Reviews*, 14 (2010) 2841-2851.
- [7] Y. Calzavara, C. Jousset-Dubien, G. Boissonnet, S. Sarrade, Evaluation of biomass gasification in supercritical water process for hydrogen production, *Energy Conversion and Management* 46 (2005) 615-631.
- [8] Y. Li, L. Guo, X. Zhang, H. Jin, Y. Lu, Hydrogen production from coal gasification in supercritical water with a continuous flowing system, *International Journal of Hydrogen Energy*, 35 (2010) 3036-3045.
- [9] A. Kruse, Supercritical water gasification, *Biofuels, Bioprod. Biorefin.*, 2 (2008) 415-437.
- [10] A. Kruse, E. Dinjus, Hydrogen from Methane and Supercritical Water, *Angewandte Chemie International Edition*, 42 (2003) 909-911.
- [11] M. H. Ansari, S. Jafarian, A. Tavasoli, A. Karimi, M. Rashidi, Hydrogen rich gas production via nano-catalytic pyrolysis of bagasse in a dual bed reactor, *Journal of Natural Gas Science and Engineering*, 19 (2014) 279-286.
- [12] A. Sharma, H. Nakagawa, K. Miura, Uniform dispersion of Ni nano particles in a carbon based catalyst for increasing catalytic activity for CH₄ and H₂ production by hydrothermal gasification, *Fuel*, 85 (2006) 2396-2401.
- [13] L. Zhang, P. Champagne, C. Xu, Screening of supported transition metal catalysts for hydrogen production from glucose via catalytic supercritical water gasification, *International Journal of Hydrogen Energy*, 36 (2011) 9591-9601.
- [14] L. He, H. Berntsen, E. Ochoa-Fernandez, J. C. Walmsley, E. A. Blekkan, D. Chen, Co-Ni Catalysts Derived from Hydrotalcite-Like Materials for Hydrogen Production by Ethanol Steam Reforming, *Topics in Catalysis*, 52 (2009) 206-217.
- [15] D. San-Jose- Alonso, J. Juan-Juan, M. J. Illan-Gomez, M. C. Roman-Martinez, Ni, Co and bimetallic Ni-Co catalysts for the dry reforming of methane, *Applied Catalysis.*, 371(2009) 54-59.
- [16] M. H. Youn, J. G. Seo, P. Kim, I. K. Song. Role and effect of molybdenum on the performance of Ni-Mo/ γ -Al₂O₃ catalysts in the hydrogen production by auto-thermal reforming of ethanol. *Journal of Molecular Catalysis A-Chemical* 261 (2007) 276-81.
- [17] L. H. Huang, J. Xie, R. R. Chen, D. Chu, A. T. Hsu, Nanorod alumina-supported Ni-Zr-Fe/Al₂O₃ catalysts for hydrogen production in auto-thermal reforming of ethanol, *Materials Research Bulletin*, 45(2010) 92-96.
- [18] S. Li, Y. Lu, L. Guo, X. Zhang, Hydrogen production by biomass gasification in supercritical water with bimetallic Ni-M/ γ Al₂O₃ catalysts (M = Cu, Co and Sn), *International Journal of Hydrogen Energy*, 36 (2011) 14391-14400.
- [19] F. L. P. Resende, P. E. Savage, Effect of Metals on Supercritical Water Gasification of Cellulose and Lignin, *Industrial and Engineering Chemistry Research* 49 (2010) 2694-2700.